Immunity, Vol. 14, 135–143, February, 2001, Copyright ©2001 by Cell Press

Increased TCR Avidity after T Cell Activation: A Mechanism for Sensing Low-Density Antigen

Tarek M. Fahmy,*†§ Joan Glick Bieler,* Michael Edidin,*‡ and Jonathan P. Schneck*§
*Department of Pathology and Medicine
Division of Immunopathology
†Department of Biophysics and Biophysical Chemistry
‡Department of Biology
Johns Hopkins University
Baltimore, Maryland 21218

Summary

While activated T cells are known to have enhanced biological responses to antigen stimulation, the biophysical basis of this increased sensitivity remains unknown. Here, we show that, on activated T cells, the TCR avidity for peptide-MHC complexes is 20- to 50-fold higher than the TCR avidity of naive T cells. This increased avidity for peptide-MHC depends on TCR reorganization and is sensitive to the cholesterol content of the T cell membrane. Analysis of the binding data indicates the enhanced avidity is due to increases in cross-linking of TCR on activated T cells. Activation-induced membrane (AIM) changes in TCR avidity represent a previously unrecognized means of increasing the sensitivity of activated T cells to small amounts of antigen in the periphery.

Introduction

Control of the dynamic range of physiological responses is a central biological process. In the T cell immune response, physiologic states of activation are associated with changes in the dynamic range of responsiveness. Thus, naive T cells require high levels of antigen and are absolutely dependent on costimulation for biological responses. In contrast, activated and memory T cells respond to lower amounts of antigen with enhanced biological responses and are relatively independent of costimulation. Activated and naive T cells have been distinguished by a number of biochemical and biological response changes (Iezzi et al., 1995; Dubey et al., 1996; Hayashi et al., 1998), including changes in membrane organization and redistribution of signaling molecules in the plane of the plasma membrane (Simons and Ikonen, 1997; Xavier et al., 1998; Montixi et al., 1998; Viola et al., 1999; Janes et al., 2000; van der Merwe et al., 2000). However, little attention has been given to comparing the organization of the membranes of naive and activated cells and its subsequent effect on the binding of antigen-MHC complexes on antigen-presenting cells (APC).

The role of TCR oligomerization in T cell signaling and activation has been studied in vitro (Reich et al., 1997; Alam et al., 1999) and in vivo. Upon contact with APC, T cell receptors on CD4 cells undergo reorganization and form a large cluster at the site of interaction that has been called the immunologic synapse/SMAC (Paul and Seder, 1994; Monks et al., 1998; Dustin and Shaw, 1999; Grakoui et al., 1999). This contact region facilitates directed release of effector molecules from the T cell toward the APC. There have been a variety of estimates of the requirement for multivalent TCR complexes for optimal signaling. Recent studies have indicated that as few as two antigen-MHC complexes are sufficient for generating all the qualitative TCR signals and that additional complexes only have quantitative effects on signaling (Bachmann et al., 1998; Bachmann and Ohashi, 1999; Cochran et al., 2000).

While the studies cited indicate a role for TCR clustering in effector functions, there has been no analysis of whether T cell receptor organization and subsequent changes in TCR avidity are modulated in different physiologic states facilitating biological responsiveness. We examined the influence of activation on the constitutive organization of T cell membrane by studying the ability of T cells to bind divalent peptide-MHC complexes. Increased binding of peptide-MHC dimers to activated T cells was apparent at both 4°C as well as at 37°C. The TCR on activated T cells was readily cross-linked by soluble dimeric MHC I molecules, increasing the overall binding affinity (avidity) of the TCR for peptide-MHC complex ~50-fold at 4°C and between 10- to 20-fold at 37°C compared to naive T cells. This enhanced avidity for peptide-MHC dimers was dependent on the membrane reorganization of the TCR, which was blocked by anti-TCR mAb, and on the cholesterol content of the cell membrane. Avidity changes in the TCR upon cell activation would alter initial T cell interaction with target cells. Hence, activation-induced TCR reorganization precedes and likely facilitates the formation of the large aggregates of TCR observed in the immunologic synapse and activation clusters (Monks et al., 1998; Grakoui et al., 1999). Avidity changes in the TCR represent a previously unrecognized means of increasing the sensitivity of activated T cells to small amounts of antigen in the periphery.

Results and Discussion

The influence of T cell activation on the organization of the T cell antigen receptor was studied by equilibrium binding of fluorescently conjugated, genetically engineered, soluble divalent MHC complexes (MHC-Ig) (Schneck et al., 2000a, 2000b). The model system studied was the murine class I restricted $CD8^+$ 2C T cell response that recognizes the peptide, SIY, presented by the syngeneic murine class I H-$2K^b$ MHC, and the peptide, QL9, presented by the allogeneic murine class I H-$2L^d$ MHC (Sykulev et al., 1994; Udaka et al., 1996).

A direct binding assay was developed to measure the binding of MHC dimers. In this assay, T cells, activated or naive, were incubated with varying amounts of fluorescently labeled MHC-Ig dimers (F:P~1:1), and binding was measured by flow cytometry. Mean channel fluores-

§To whom correspondence should be addressed (e-mail: tarekf2000@yahoo.com [T. M. F.], jschneck@welchlink.welch.jhu.edu [J. P. S.]).

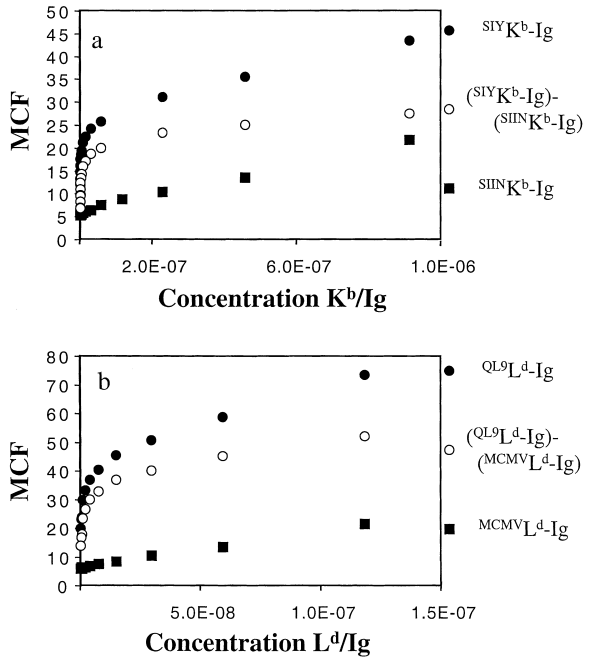

Figure 1. Specific Binding of MHC Dimers to Activated 2C T Cells

MHC dimers were purified to homogeneity using size exclusion chromatography. Dimers were fluorescently labeled with fluorescein isothiocyanate (FITC) at pH 7.4 to target the amino termini, loaded with peptide, and then purified once more by size exclusion. Labeled MHC-Ig dimers were incubated with T cells for 1–2 hr at 4°C, and binding was measured by flow cytometry. There were no washing steps prior to flow cytometric analysis. Mean channel fluorescence (MCF) value was a measure of the amount of bound ligand. (A) Binding of labeled K^b-Ig loaded with (SIY)-SIYRYYGL, $^{SIY}K^b$-Ig (closed circles), to activated T cells. Nonspecific binding was determined using K^b-Ig loaded with the K^b-specific peptide derived from ovalbumin-SIINFEKL (closed squares). Specific binding (open circles) was calculated by subtracting nonspecific binding from total binding. (B) Binding of L^d-Ig loaded with (QL9)-QLSPFPFDL, $^{QL9}L^d$-Ig (closed circles), to activated T cells. Nonspecific binding was determined using L^d-Ig loaded with the L^d-restricted peptide derived from MCMV-YPHFMPTNL (closed squares). Specific binding (open circles) was calculated by subtracting nonspecific binding from total binding.

cence (MCF) value was a measure of the amount of bound dimeric MHC ligand. Specific binding was determined by subtracting nonspecific binding, binding of noncognate peptide-MHC-Ig complex (either SIIN loaded K^b-Ig complexes [$^{SIIN}K^b$-Ig] or MCMV loaded L^d-Ig complexes [$^{MCMV}L^d$-Ig]), from the total binding of cognate peptide MHC-Ig ($^{SIY}K^b$-Ig or $^{QL9}L^d$-Ig) to T cells (Figure 1).

Activated T Cells Bind MHC-Dimers Differently than Naive T Cells

Peptide-loaded MHC dimers, $^{SIY}K^b$-Ig, bound to activated T cells at 4°C with a different concentration dependence than when they bound to naive T cells (Figure 2A). This difference was also seen for the peptide-MHC complex, $^{QL9}L^d$-Ig (Figure 2C). Peptide-loaded MHC dimers also bound to activated T cells with a different concentration dependence than to naive T cells at 37°C (Figures 3A and 3C). The difference between activated and naive cells is highlighted at low concentrations of ligand where in each case activated T cells bound more dimeric MHC than naive T cells. Scatchard analysis showed a striking difference between the binding of dimeric peptide-MHC to activated and naive T cells. Scatchard plots of peptide-MHC dimer binding to activated T cells were curvilinear. This marked curvilinearity was not seen with MHC dimer binding to naive T cells (Figures 2B and 2D). The Scatchard plot for naive cells was linear, indicating uniform binding sites. The curvilinear Scatchard plot implied a more complex binding interaction between TCR and peptide-MHC complexes on activated cells. Scatchard plots of peptide-MHC dimer binding at 37°C to activated T cells were also curvilinear (Figures 3B and 3D). Thus, binding differences between activated and naive T cells were apparent whether binding was done at 4°C or 37°C.

Curvilinearity in a Scatchard plot may be due to a number of different molecular mechanisms (Wofsy and Goldstein, 1992). One possible mechanism is that activated T cells have acquired a second independent site that binds MHC with a different affinity than the TCR of naive cells. A second mechanism consistent with a curvilinear Scatchard plot is negative cooperativity; binding of ligand to one TCR lowers the affinity of other TCRs for another ligand molecule. Finally, the curvilinear Scatchard plot could be due to increased T cell receptor cross-linking on activated T cells leading to an increased avidity for dimeric MHC-Ig. To distinguish among these possibilities, we generated Fab fragments from K^b-Ig. If the difference between the binding of K^b-Ig to activated and naive T cells was due to either a second class of binding sites or negative cooperativity, one would expect to see this difference in the binding of monomeric K^b-Ig Fab fragments. If, however, the difference observed was due to receptor cross-linking, one would not expect to see a difference between activated and naive T cells in MHC monomer binding experiments. The binding isotherms of $^{SIY}K^b$-Ig-Fab were virtually identical for activated and naive T cells (Figure 2E). Hence, the curvilinear Scatchard plots are likely due to a change in TCR organization between naive and activated T cells that facilitates binding of MHC-dimer complex to activated T cells.

Activation Changes TCR Membrane Organization

Changes in the local receptor density after cell activation could change the avidity of dimeric MHC (DeLisi and Chabay, 1979; Lauffenburger and Linderman, 1993; Bray et al., 1998). To disperse any local concentrations of receptor and to prevent ligand-induced cross-linking, we studied binding of MHC dimer in the presence of an antibody Fab specific for the Cβ domain of murine αβ TCR, H57 (Kubo et al., 1989). H57 recognizes a conserved site in the Cβ domain of murine TCR (Wang et al., 1998) (Figure 4E) distinct from the interaction site of TCR for cognate peptide-MHC complexes. This suggested the use of H57 as a "molecular fender," to prevent the close apposition of one TCR to another. The binding of MHC-Ig to immobilized TCR, measured by surface plasmon resonance (SPR), was not affected by prebinding 2C TCR with H57 Fab fragments (Figure 4F). Therefore, functionally there is no steric inhibition between TCR and peptide-MHC due to H57 binding.

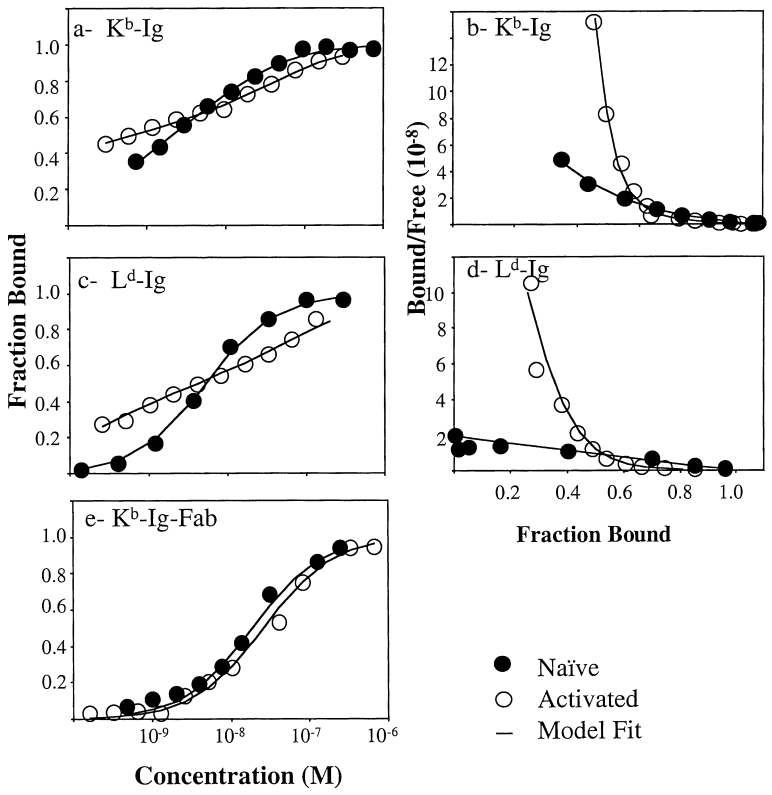

Figure 2. Activated T Cells Bind MHC-Dimers Differently than Naive T Cells

MHC monomers, however, bind with the same concentration dependence to both activated and naive 2C T cells. (A–D) MHC dimers were purified and used in flow cytometry experiments as described above. Labeled MHC-Ig dimers were incubated with T cells for 2 hr at 4°C. Mean channel fluorescence (MCF) value was a measure of the amount of bound ligand. Nonspecific binding has been subtracted as described above. Only specific binding is shown. (A) Specific binding of peptide-loaded $^{SIY}K^b$-Ig to naive (closed circles) and activated (open circles) T cells. (B) Scatchard plot of the data in (A). (C) Specific binding of peptide loaded $^{QL9}L^d$-Ig to naive (closed circles) and activated (open circles) T cells. (D) Scatchard plot of the data in (C). Lines through the data points are a nonlinear least squares fit using a dimeric ligand-monovalent receptor model (Perelson, 1984). (E) MHC monomers were prepared by papain treatment of the same MHC dimer stock (see Experimental Procedures), then fluorescently labeled with FITC, peptide loaded, and purified to size homogeneity using size exclusion. Specific binding of peptide-loaded, Fab fragments from $^{SIY}K^b$-Ig, to naive (closed circles) and activated (open circles) T cells was performed as described.

Incubation with H57 Fab had a dramatic impact on the binding of cognate $^{SIY}K^b$-Ig to activated T cells (Figures 4A and 4B). The curvilinearity seen in Scatchard plots, characteristic of $^{SIY}K^b$-Ig binding to activated cells, was significantly reduced. MHC-Ig dimer binding to H57-treated activated 2C cells appeared similar to dimer binding to naive cells. In contrast, H57 treatment had no effect on the binding of MHC-Ig dimer to naive T cells (Figures 4C and 4D). Thus, binding of a second ligand (H57 Fab), which was expected to block TCR cross-linking, reduced the avidity of MHC-Ig for TCR on activated T cells but not on naive T cells.

The ability of H57 to block cross-linking of TCR may have implications for the configuration of TCR on naive versus activated T cells. The size of the Fab fragment of H57 is ~70 Å (Figure 4E). At this size, H57 could readily block the interaction of dimeric MHC with two TCRs within a single CD3 unit. Several investigators

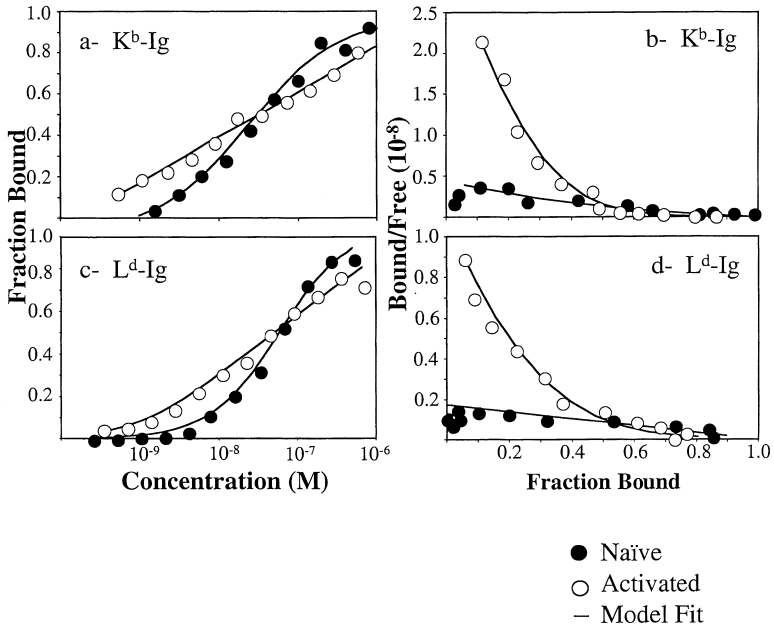

Figure 3. MHC Dimers Bind Activated 2C T Cells with Different Concentration Dependence than Naive 2C T Cells at Physiologic Temperatures

(A–D) MHC dimers were purified and used in flow cytometry experiments as described above. Labeled MHC-Ig dimers were incubated with T cells for 20–30 min at 37°C. Azide, 0.05%, was used to inhibit internalization of dimer in all experiments performed at 37°C. Mean channel fluorescence (MCF) value was a measure of the amount of bound ligand. (A) Specific binding of peptide-loaded, $^{SIY}K^b$-Ig, to naive (closed circles) and activated (open circles) T cells. (B) Scatchard plot of the data in (A). (C) Specific binding of peptide loaded $^{QL9}L^d$-Ig to naive (closed circles) and activated (open circles) T cells. (D) Scatchard plot of the data in (C). Lines through the data points are a nonlinear least squares fit using a dimeric ligand-monovalent receptor model (Perelson, 1984).

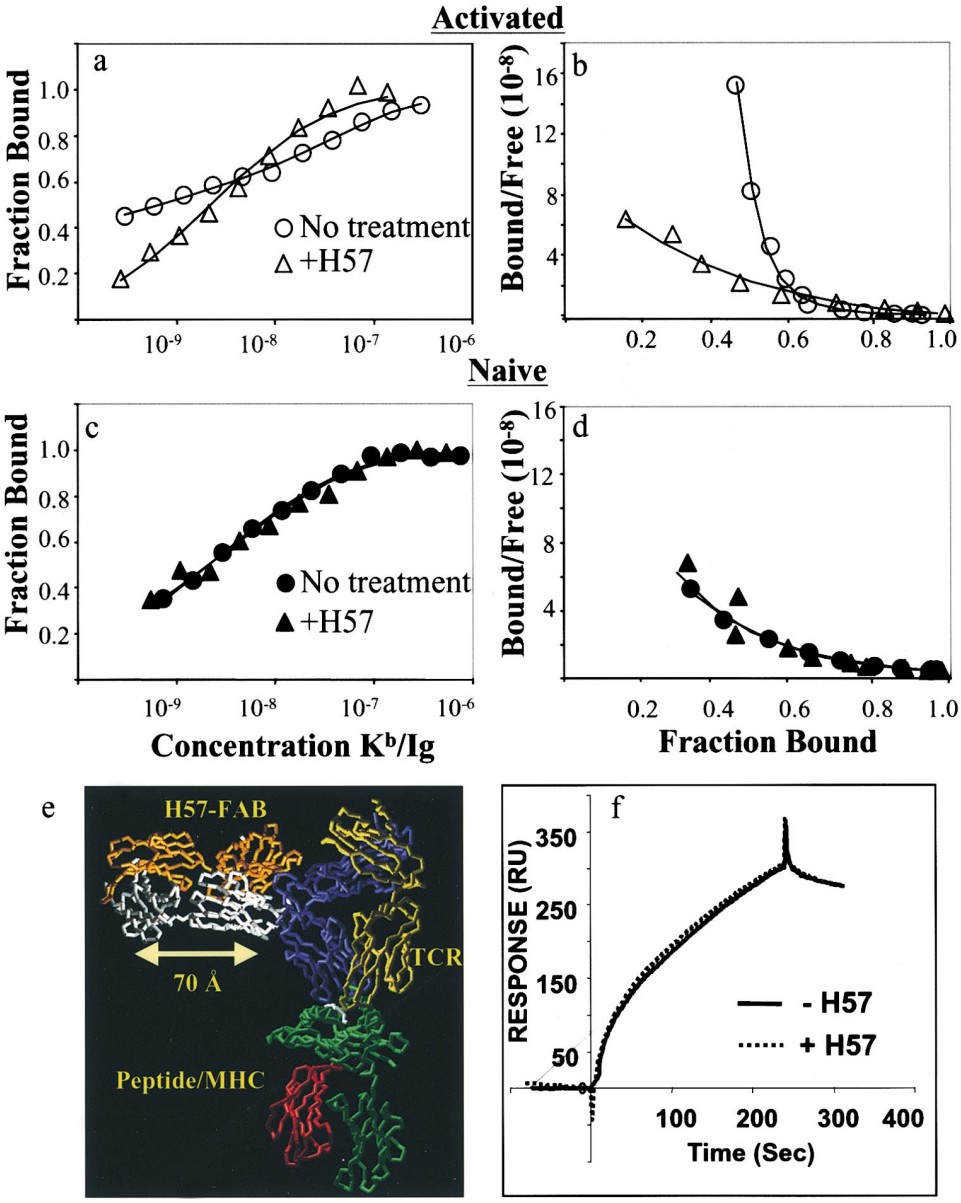

Figure 4. H57-Fabs Influence the Binding of MHC Dimer to Activated T Cells but Not Naive T Cells

(A and C) $^{SIY}K^b$-Ig dimer binding to naive (closed) and activated (open) T cells in the presence (triangles) and absence (circles) of H57 Fab. Cells were pretreated with saturating amounts of H57 Fabs, prepared by papain fragmentation (Pierce Immunopure Fragmentation Kit) of H57 antibody (Pharmingen), and then washed twice followed by titration of $^{SIY}K^b$-Ig.

(B and D) Scatchard plots of (A) and (C).

(E) A model of the three-dimensional structure of the αβ 2C TcR heterodimer complexed with H57 Fab in the presence of peptide/K^b complex. The three-dimensional structure was obtained for N15 αβ TCR in complex with H57-Fab (Wang et al., 1998). There is considerable homology with the constant region of the 2C αβ TCR. Thus, the crystal structure of the complex of pep/Kb-2C TCR (Garcia et al., 1996a) was superimposed on the structure of N15 TCR using Swiss PdbViewer ver. 3.0.

(F) Treatment of 2C TCR with H57 Fabs does not interfere with its binding to MHC. Surface plasmon resonance (Biacore) comparison of $^{SIY}K^b$-Ig-FITC binding to untreated 2C TCR (solid line) and 2C TCR treated with saturating amounts of H57 Fab (dashed line). TCR was immobilized onto the surface of a CM5 Biacore chip at ~1000 RU. $^{SIY}K^b$-Ig was then flowed over the surface for 4 min at 5 μl/min to establish the binding profile in the absence of H57. Next, H57 Fab at 10 mM was flowed over the surface for 5 min and saturation of TCR with H57 was confirmed. $^{SIY}K^b$-Ig was then flowed over the surface once more for 4 min at 5 μl/min to establish its binding profile after H57 had bound TCR.

have reported that the functional signaling CD3 complex consists of two TCR within the same CD3 complex (Exley et al., 1995; Fernandez-Miguel et al., 1999). Because of distance constraints, it seems less likely that H57Fab would inhibit two TCR in separate CD3 complexes. Thus, our findings suggest that the TCR-CD3 complex may contain two αβ dimer units in activated T cells, while this is not necessarily the case in naive T cells.

Recent studies have shown that the immunologic synapse/SMAC can form even in the presence of H57 anti-

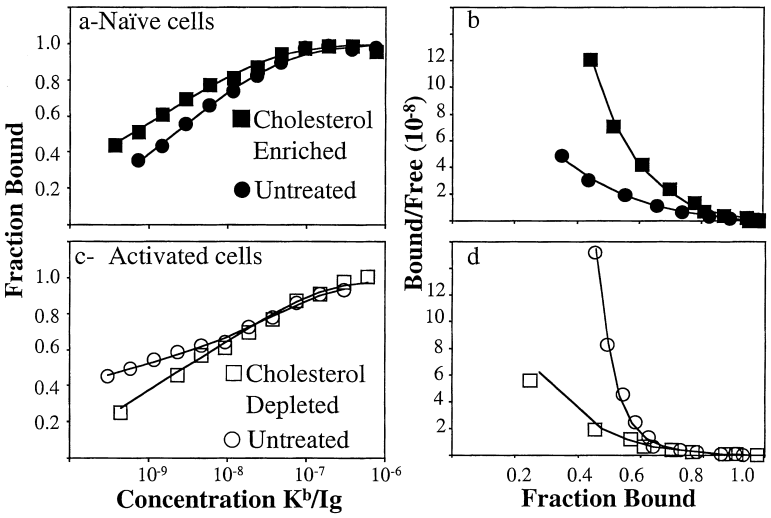

Figure 5. Cholesterol Affects the Binding of MHC Dimer to T Cells

(A and B) Cholesterol enrichment of naive cells and its effects on (A) binding isotherms and (B) Scatchard plots of $^{SIY}K^b$-Ig binding. Naive cells (closed circles) were pretreated with methyl-β-cyclodextrin-cholesterol inclusion complexes (0.7–0.9 mM) (closed squares) and assayed for binding of $^{SIY}K^b$-Ig.

(C and D) Cholesterol depletion of activated T cells and its effects on (C) binding isotherm and (D) Scatchard plot of $^{SIY}K^b$-Ig binding. Activated cells (open circles) were pretreated with 30 mM methyl-β-cyclodextrin (open squares) for 30 min at 37°C and assayed for binding of $^{SIY}K^b$/Ig.

bodies (Dustin and Cooper, 2000). Here, we demonstrate that H57 Fab blocked the enhanced binding of dimeric MHC to activated T cells. This finding serves to highlight distinctions between the immunologic synapse/SMAC and increased binding of MHC dimers to activated T cells. Additional studies will further enhance our understanding of the relationship between activation-induced changes in membrane (AIM) TCR organization detected by MHC dimer binding and formation of the immunologic synapse/SMAC.

TCR Avidity Is Influenced by Membrane Cholesterol

One of the major consequences of cellular activation is the compartmentalization of TCR and signaling molecules in operationally defined membrane lipid rafts (Simons and Ikonen, 1997; Montixi et al., 1998; Xavier et al., 1998; Viola et al., 1999; Janes et al., 2000; van der Merwe et al., 2000). These lipid rafts are commonly isolated as glycosphingolipid and cholesterol-rich fractions of membrane extracts (Brown and London, 1998). Rafts are dispersed when membrane cholesterol levels are reduced (Kabouridis et al., 2000). To see if the enhanced binding of MHC dimers observed following T cell activation depended upon plasma membrane cholesterol content, we manipulated cholesterol levels (Gimpl et al., 1997) in naive and activated cells. Addition of cholesterol to naive T cells enhanced the avidity of dimeric MHC-Ig for TCR (Figure 5A). When cholesterol was added to naive cells, the slope of the Scatchard plot increased and became more curvilinear than that for untreated naive cells (Figure 5B). Conversely, depletion of cholesterol from activated cells reduced the avidity of MHC dimer binding (Figure 5C) and was reflected in a change in the Scatchard plot that was less curvilinear (Figure 5D). Treatment of activated cells with *sphingomyelinase*, an enzyme that cleaves *sphingomyelin,* another important component in rafts, also reduced the avidity of dimer binding (data not shown). Thus, the changes in binding seen in activated T cells are consistent with a cholesterol-dependent membrane reorganization of the TCR that affects its potential for dimerization. This is also consistent with the previous data (Figures 4A and 4B) showing that H57 Fab treatment lowered the avidity for dimeric MHC.

Activated Cells Have an Enhanced Ability to Cross-Link TCR

Our experiments indicated that the changes in binding of MHC-Ig dimer to TCR observed for activated T cells are likely due to increased cross-linking of TCR leading to an increased avidity for dimeric MHC-Ig complex. To quantitate cross-linking, binding data were fit to a model of equilibrium dimerization of homogeneous monovalent receptors by divalent ligand (Perelson, 1984) (Figure 6A). In this model, the first monovalent binding event creates a complex that increases the local concentration of receptors. Since it is assumed that all receptors are identical, the second binding event increases the "apparent binding affinity," i.e., the avidity. Parameters in this model are (1) the single site dissociation constant, K_d, which characterizes the binding of one site on the MHC-Ig to one TCR, and (2) the dimensionless cross-linking constant, K_xR_t, which characterizes the ability of the MHC/TCR complex to recruit another TCR. Binding avidity, K_v, is approximately the ratio K_d/K_xR_t (Lauffenburger and Linderman, 1993). In cases where there is minimal cross-linking potential, K_xR_t is close to 1 and there is little difference between K_d and K_v. Where the cross-linking potential K_x is high, there is an enhancement of binding due to dimerization, resulting in a measured avidity stronger than the intrinsic single site affinity.

Analysis of the binding data indicated that the overall avidity, K_v, of the dimeric MHC for activated cells was ~50-fold higher than for naive cells at 4°C and ~15- to 20-fold higher than for naive cells at 37°C (Table 1). The increased avidity of MHC-Ig binding on activated T cells is due to an increased cross-linking constant (K_x), rather than an increased intrinsic dissociation constant (K_d) (Table 1). The increase in avidity seen cannot be accounted for by changes in total amount of TCR. TCR levels increase ~2-fold on activated cells as assayed by both dimer staining (Table 1) and by 1B2, anticlonotypic mAb, staining (data not shown). Cell surface CD8 levels also did not change significantly (data not shown). Thus,

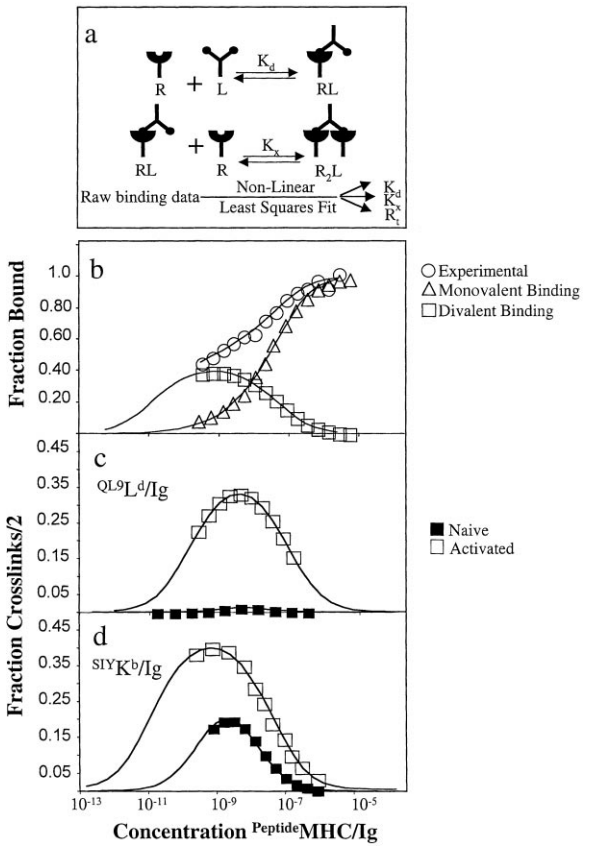

Figure 6. A Model of Dimeric Ligand Binding to Monomeric Receptors

(A) Initially a divalent ligand, [L], binds with one site to a receptor [R]. This singly bound dimer, [RL], can bind to another receptor in its vicinity to form a doubly bound complex [R_2L]. The equilibrium parameters describing this binding are the intrinsic single site dissociation constant, K_d, the equilibrium cross-linking constant, K_x, the total number of receptors bound, R_t. The dimensionless cross-linking equilibrium constant is defined as K_xR_t. These parameters were obtained by nonlinear fits of the binding data to the equilibrium solution of this model (Perelson, 1984). Adequacy of fit was judged by a reduced chi-square of 1.5 or less and randomized residuals. The quantity K_xR_t is the factor by which total ligand binding is enhanced by divalent binding (receptor cross-linking). The avidity of the interaction, accentuated at low dimer concentrations, is estimated from K_d/K_xR_t.

(B) Deconvolution of dimer binding data (open circles) into single (open triangles) and double bound species (open squares) (cross-linking curve) for $^{SIY}K^b$-Ig binding to activated cells. Deconvolution was performed by substituting the fitted parameters into the single and double bound species equations (see Experimental Procedures). Points on those curves refer to the experimental range over which the binding experiment was performed.

(C and D) Cross-linking curves for (C) $^{SIY}K^b$-Ig and (D) $^{QL9}L^d$-Ig.

the enhanced avidity observed is not due to either changes in CD8 or TCR levels but results from an increase in the cross-linking potential.

The intrinsic affinity, K_d, estimated by this study highlights the importance of using the full TCR, consisting of both the TCR α/β complex and CD8 coreceptor, to estimate affinity of interaction. In our experiments, the single site interactions, K_d, were 1–4 nM for $^{SIY}K^b$ and ~10 nM for $^{QL9}L^d$ complexes at 4°C. The affinity estimated previously in surface plasmon resonance (SPR) experiments using soluble 2C TCR for $^{QL9}L^d$ was 3.9 μM and for $^{SIY}K^b$ was 32 μM (Garcia et al., 1997). Two notable differences can explain this apparent discrepancy. First, SPR estimates of the affinity of 2C for $^{QL9}L^d$ and $^{SIY}K^b$ were performed in the absence of CD8 binding. CD8 is clearly an important factor that contributes to the intrinsic affinity measured (Garcia et al., 1996b; Sykulev et al., 1998; Wyer et al., 1999; Daniels and Jameson, 2000). Second, temperature is a recognized variable that impacts on affinity (Willcox et al., 1999). Measuring K_d values at higher temperatures results in a weaker affinity, usually due to an increase in off-rate. Higher temperatures also increase the rate of loss of cross-links, cross-link off-rate. As a result, the overall avidity decreases. Physiologically, this effect of temperature on the avidity can be compensated for by multivalent antigen/MHC complexes on the APC. Recent studies indicate that antigen on APC may be clustered in raft-like structures (Anderson et al., 2000). The multivalent character of these structures also could facilitate recognition of antigen by activated T cells. Our measurements are quite consistent with values obtained where CD8 is physiologically associated with the TCR. Considering differences in temperature, our measurements of 10 nM for $^{QL9}L^d$ at 4°C were very close to the previously reported intrinsic affinity of 50 nM for $^{QL9}L^d$ complexes at 25°C (Sykulev et al., 1998). Sykulev et al. also found the affinity of $^{SIY}K^b$ was ~100 nM at 25°C. Our findings for the K_d intrinsic affinity of 1 nM at 4°C and 65 nM at 37°C for $^{SIY}K^b$, using the MHC dimers, are quite consistent with the previous determinations where CD8 also contributes to the binding interaction. The K_d values are based on a monovalent receptor-divalent ligand model (Perelson, 1984). Although other models could be applied and might impact on estimated single site K_d, the data presented here fit this model very well.

The estimated K_v correlate well with the known biological activities of the different cognate TCR ligands. 2C CTL mediate lysis of target cells pulsed with as little as picomolar amounts of SIY peptide and yet require larger amounts of QL9 peptides (Schlueter et al., 1996; Udaka et al., 1996; Garcia et al., 1997). Previously, by measuring the K_d alone, 3.9 μM for QL9-L^d and 32 μM for SIY-K^b, one was unable to explain why the $^{SIY}K^b$ complex appears to be a more potent agonist than the $^{QL9}L^d$ complex (Garcia et al., 1997). The estimated K_v for $^{SIY}K^b$-Ig was 18 pM at 4°C and 3.2 nM at 37°C, and for $^{QL9}L^d$-Ig, 0.28 nM at 4°C and 11.2 nM at 37°C. Thus, the avidity, a parameter characterizing the physical event of multivalent ligand/receptor binding, was more consistent with the potency of $^{SIY}K^b$ and $^{QL9}L^d$ in stimulating biological responses than the K_d.

As seen schematically in Figure 6A, dimeric MHC complexes can bind with one arm to one receptor, RL, or with both arms to two receptors, R_2L. The dimeric MHC-Ig binding isotherms (Figures 2 and 3) are the sum of both singly bound, RL, and doubly bound, R_2L, components. By deconvolution of the binding isotherms into singly bound and doubly bound components (Figure 6B), we were able to estimate the number of TCR cross-links, i.e., the number of doubly bound MHC-Ig complexes. At lower concentrations, binding is dominated by the doubly bound component of the isotherm, R_2L.

Table 1. Summary of Model Fit Parameters

		Temperature = 4°C				
		K_D (nM)	K_X (Cell/#)	R_T (# MCF)	K_XR_T	K_V (nM)
Naive	K^b/Ig-SIY	4.2 ± 1	0.12 ± 0.05	36 ± 4	4.4 ± 1	1.0 ± 0.4
Act.	K^b/Ig-SIY	1.3 ± 0.5	2.6 ± 0.1	28 ± 5	73 ± 4	0.018 ± .002
Naive	L^d/Ig-QL9	10.7 ± 1	0.005 ± 0.001	20 ± 3	1.0 ± 0.1	10.7 ± 1
Act.	L^d/Ig-QL9	7.3 ± 2	0.43 ± 0.1	60 ± 10	26 ± 7	0.28 ± 0.09
		Temperature = 37°C				
		K_D (nM)	K_X (Cell/#)	R_T (# MCF)	K_XR_T	K_V (nM)
Naive	K^b/Ig-SIY	77 ± 10	0.03 ± 0.01	47 ± 6	1.4 ± 0.2	55 ± 11
Act.	K^b/Ig-SIY	64 ± 8	0.21 ± 0.2	95 ± 10	20 ± 5	3.2 ± 0.5
Naive	L^d/Ig-QL9	116 ± 10	ND	54 ± 7	ND	116 ± 10
Act.	L^d/Ig-QL9	100 ± 9	0.07 ± 0.02	127 ± 20	8.9 ± 3	11.2 ± 3

K_d is the single site equilibrium dissociation constant. K_x is the equilibrium cross-linking constant with units of inverse number of receptors per cell. R_t is the total number of receptors available for binding in mean channel fluorescence (MCF) unit equivalents. K_xR_t is a dimensionless quantity. K_v is the avidity at low dimer concentrations, which is estimated as $K_v \sim K_d/K_xR_t$ (Lauffenburger and Linderman, 1993). Values shown are derived from fits to 4°C and 37°C dimer binding data, respectively (Figure 2). Indicated errors are standard errors calculated based on the model fit. ND indicates that the values of the equilibrium cross-linking constant from the model fit were too insignificant to tabulate accurately. As a result, the avidity constant was not different from the instrinsic affinity constant.

At higher concentrations, monovalent binding, RL, dominates because of competition for available receptors. The intersection of both profiles defines the maximum number of cross-links. Using this approach, we found that the maximum number of cross-links formed on activated cells was greater than those formed on naive T cells (Figures 6C and 6D). On activated T cells, ~75% of the TCR were cross-linked by ^{QL9}Ld-Ig and 80% of the TCR were cross-linked by $^{SIY}K^b$-Ig. Naive cells showed significantly less cross-linking; <5% were cross-linked by $^{QL9}L^d$-Ig and 35% were cross-linked by $^{SIY}K^b$-Ig.

Oligomerization, specifically dimerization of TCR, has been observed experimentally in vitro (Reich et al., 1997; Alam et al., 1999). In those systems, oligomerization was either concentration or temperature dependent and not studied in the setting of the intact cellular plasma membrane. Our studies indicate that dimerization potential is controlled by different physiologic states and influenced by membrane cholesterol. These findings may offer a biologic context for the previous in vitro findings.

Recently, several groups have reported that the average affinity of TCR for peptide/MHC complexes increases upon secondary immunization (Busch et al., 1999; Rees et al., 1999; Savage et al., 1999). This process has been attributed to the preferential outgrowth of higher affinity T cells present in the primary T cell population and may reflect competition for antigen by the T cell population (Kedl et al., 2000). In light of our findings that TCR avidity is dependent on the physiologic state of activation, it is also possible that these results are, at least in part, due to different physiologic states of activation. Thus, in analyzing affinities/off-rates of populations of T cells it is also important to account for their physiologic state of activation.

The increased number of cross-links observed on activated T cells indicates that these cells cluster TCR more efficiently than naive cells. This is consistent with observations that oligomers tend to form at a contact site between the APC and effector T cells during activation, i.e., at an "immunological synapse," where a specific pattern of receptor segregation is observed (Monks et al., 1998; Grakoui et al., 1999). Greater number of TCR cross-links on activated T cells could facilitate an efficient formation of the immunological synapse by active transport processes (van der Merwe et al., 2000). Conversely, the formation of these oligomers at the APC contact site suggests TCR cross-linking in T cell activation (Bachmann and Ohashi, 1999).

Conclusion

In vivo, the effective clearing of antigen-MHC complexes is hampered by both the low intrinsic affinity of TCR for peptide/MHC complex (Davis et al., 1998) and the low densities of antigen-MHC on target cells (Sykulev et al., 1996). Our findings indicate that T cells have developed a unique ability to accommodate both of these barriers. Activation-induced membrane TCR reorganization leading to increased avidity allows T cells with intrinsically low affinity to bind multimeric MHC complexes with a substantially higher avidity. This leads to more efficient recognition of low-density antigen-MHC complexes, which is clearly important for sensitive and effective signaling by activated cells. This mechanism could also ensure that T cells do not break tolerance and cause autoimmune response by preventing premature activation of naive cells. Furthermore, enhanced avidity may permit interactions of long duration in the absence of affinity maturation such as occurs in B cells. Thus, the enhanced avidity of activated T cells may be a general mechanism for promoting efficient cell signaling and represents an early mechanism of immunomodulation.

Experimental Procedures

Generation of Naive and Activated 2C T Cells

Naive T cells were isolated from 2C mouse splenocytes. $CD8^+$ cells were enriched to >95% purity using a $CD8^+$ T cell subset enrichment column (R&D Systems MCD8C-1000). A portion of the naive 2C T cells were then activated in vitro with irradiated allogeneic splenocytes from Balb/C mice (Jackson Labs) in RPMI media with 10% fetal calf serum (Hyclone). The ratio of naive T cells to irradiated splenocytes used was in the range 1.5–2.0. Activated cells were used for binding studies of 4–7 days poststimulation.

Preparation of Fluorescently Labeled MHC Dimers and Monomers

Soluble MHC-Ig fusion proteins were generated by genetically fusing the extracellular domain of a class I MHC to the amino termini of the immunoglobulin heavy chain (IgG1) (Dal Porto et al., 1993; Schneck et al., 2000a, 2000b; Slansky et al., 2000). The result was a dimeric MHC-Ig complex with the Ig as a molecular scaffold for the MHC. These MHC-Ig complexes were fluorescently labeled with fluorescein isothiocyanate (FITC) (Molecular Probes) at pH 7.4 and purified to size homogeneity using size exclusion chromatography (Amersham Pharmacia Biotech) and then loaded with peptide (Macromolecular Resources). Labeled dimer had a fluorescein/protein ratio of 1–2 because of preferential labeling at the amino termini of the complex at pH 7.4. Fluorescent labeling did not affect the binding properties of MHC-Ig as assessed by a surface plasmon resonance (Biacore) binding assay (data not shown). In brief, 2C TCR was immobilized on the surface of a biosensor chip and MHC-Ig was flowed on the sensor surface. Binding profiles of labeled and unlabeled MHC-Ig were identical. MHC monomers were prepared from the same dimer stock by papain treatment of MHC-Ig and purified as described (Pierce Immunopure Fab preparation kit). Preparation of MHC-Ig Fab fragments by papain treatment yielded functionally active protein that specifically bound TCR immobilized to the surface of a biosensor (Biacore) (data not shown).

Peptide Loading of MHC-Ig Complexes

Peptide loading of MHC-Ig was performed as described previously (Schneck, 2000b). K^b-Ig complexes were efficiently loaded by a brief alkaline stripping (150 mM NaCl and 15 mM Na_2CO_3 [pH 11.5]) procedure, followed by a slow refolding step at neutral pH in the presence of 40-fold molar excess of peptide. Peptide stripping of L^d-Ig dimers was performed under mildly acidic conditions (citrate-phosphate buffer, pH to 6.5) in the presence of 40-fold molar excess peptide and 2-fold molar excess β_2-microglobulin. Using a conformationally sensitive ELISA, we have estimated that $>$90% of the K^b-Ig and L^d-Ig dimers were folded properly. Using fluorescently tagged peptides, we also determined that greater than 95% of the MHC is loaded with the peptides of interest (data not shown).

Binding Assay of MHC Dimers and Monomers

Binding of peptide loaded, fluorescently labeled MHC-Ig dimers and monomers was measured by flow cytometry using a FACScalibur (Becton Dickinson). In this assay, T cells, activated or naive, were incubated with varying amounts of fluorescently labeled MHC-Ig dimers (F:P$\sim$1:1), and binding was measured by flow cytometry. All binding experiments were performed at 4°C except where indicated otherwise. For experiments performed at 37°C, azide (0.05%) was used to inhibit internalization of dimer. There were no washing steps prior to flow cytometric analysis. Mean channel fluorescence (MCF) value was a measure of the amount of bound ligand. Data presented in experiments, Figures 2–6, are specific binding, which was calculated by subtracting nonspecific binding from total binding. These values were then normalized to the maximum specific mean channel fluorescence obtained by saturation with ligand. Typical windows for specific binding using this assay were between 20–60 MCF units.

T Cell Cholesterol Addition and Depletion

Cholesterol was added to naive cells using methyl-β-cyclodextrin-cholesterol inclusion complexes. These complexes were prepared by incubation of methyl-β-cyclodextrin (50 mg/ml) (Sigma) with a final cholesterol (Calbiochem) concentration of 3 mM in an argon atmosphere with continuous vortexing at 37°C for 24 hr. Activated cells were depleted of cholesterol by pretreatment with methyl-β-cyclodextrin, 30 mM, for 30 min at 37°C. In both cases, cells were washed twice prior to titration with labeled MHC-Ig. Cell viability was 85% or greater as determined by trypan blue staining.

Data Modeling

The equilibrium solution to the dimerization reaction is (Perelson, 1984): $[RL] = R_t\beta\ (-1+(1+4\delta)^{1/2})/2\delta$, $[R_2L] = R_t(1+2\delta-(1+4\delta)^{1/2})/4\delta$ where $\beta = 2L/(K_d+2L)$, $\delta = \beta(1-\beta)K_xR_t$. The total concentration of bound ligand is $[L_b] = [RL]+[R_2L]$ and the fraction of ligand bound is $[L_b]/R_t$. Three parameters are unknown in these equations, K_d, K_x, R_t. To determine those parameters, fits of the binding data were performed using the nonlinear fitting algorithm of Microcal Origin 4.1. The resulting three parameters, K_d, K_x, R_t were used to approximate the avidity constant at low concentration, $K_v \sim K_d/K_xR_t$, and to calculate the concentration of singly bound ligand [RL] and concentration of cross-links $[R_2L]$.

Acknowledgments

We thank L. Siew, B. Casbasag, T. Armstrong, and J. Slansky for assistance in making the MHC/Ig construct and maintenance of cell lines and mice; D. Margulies, B. Goldstein, S. Sadegh-Nasseri, L. Brand, G. Rose, and M. Paulaitis for support and helpful discussions; and S. Desiderio, B. Silicano, A. Rosen, M. Soloski, and L. Brand for reading this manuscript. Support for this work was provided by grants from the National Institutes of Health AI-29575, AI-44129, AI-14584 and NMSS (RG 2637 A2/1). For details about the Schneck lab, please see the lab home page at http://pathology2.jhu.edu/schnecklab.

Received September 25, 2000; revised January 9, 2001.

References

Alam, S.M., Davies, G.M., Lin, C.M., Zal, T., Nasholds, W., Jameson, S.C., Hogquist, K.A., Gascoigne, N.R.J., and Travers, P.J. (1999). Qualitative and quantitative differences in T cell receptor binding of agonist and antagonist ligands. Immunity *10*, 227–237.

Anderson, H.A., Hiltbold, E.M., and Roche, P.A. (2000). Concentration of MHC class II molecules in lipid rafts facilitates antigen presentation. Nat. Immunol. *1*, 156–162.

Bachmann, M.F., and Ohashi, P.S. (1999). The role of T-cell receptor dimerization in T-cell activation. Immunol. Today *20*, 568–576.

Bachmann, M.F., Salzmann, M., Oxenius, A., and Ohashi, P.S. (1998). Formation of TCR dimers/trimers as a crucial step for T cell activation. Eur. J. Immunol. *28*, 2571–2579.

Bray, D., Levin, M., and Morton-Firth, C.J. (1998). Receptor clustering as a cellular mechanism to control sensitivity. Nature *393*, 85–88.

Brown, D.A., and London, E. (1998). Functions of lipid rafts in biological membranes. Annu. Rev. Cell. Dev. Biol. *14*, 111–136.

Busch, D.H., and Pamer, E.G. (1999). T cell affinity maturation by selective expansion during infection. J. Exp. Med. *189*, 701–710.

Cochran, J.R., Cameron, T.O., and Stern, L.J. (2000). The relationship of MHC-peptide binding and T cell activation probed using chemically defined MHC class II oligomers. Immunity *12*, 241–250.

Dal Porto, J., Johansen, T.E., Catipovic, B., Parfitt, D.J., Tuveson, D., Gether, U., Kozlowski, S., Fearon, D., and Schneck, J.P. (1993). A soluble divalent class I major histocompatibility complex molecule inhibits alloreactive T cells at nanomolar concentrations. Proc. Natl. Acad. Sci. USA *90*, 6671–6675.

Daniels, M.A., and Jameson, S.C. (2000). Critical role for CD8 in T cell receptor binding and activation by peptide/major histocompatibility complex multimers. J. Exp Med. *191*, 335–346.

Davis, M.D., Boniface, J.J., Reich, Z., Lyons, D., Hampl, J., Arden, B. and Chien, Y.-h. (1998). Ligand recognition by αβ T cell receptors. Annu. Rev. Immunol. *16*, 523–544.

DeLisi, C., and Chabay, R. (1979). The influence of cell surface receptor clustering on the thermodynamics of ligand binding and the kinetics of its dissociation. Cell Biophys. *1*, 117–131.

Dubey, C., Croft, M., and Swain, S.L. (1996). Naive and effector CD4 T cells differ in their requirements for T cell receptor versus costimulatory signals. J. Immunol. *157*, 3280–3289.

Dustin, M.L., and Shaw, A.S. (1999). Costimulation: building an immunological synapse. Science *283*, 649–650.

Dustin, M.L., and Cooper, J.A. (2000). The immunological synapse and the actin cytoskeleton: molecular hardware for T cell signaling. Nat. Immunol. *1*, 23–29.

Exley, M., Wileman, T., Mueller, B., and Terhorst, C. (1995). Evidence for multivalent structure of T-cell antigen receptor complex. Mol. Immunol. *32*, 829–839.

Fernandez-Miguel, G., Alarcon, B., Iglesias, A., Bluethmann, H., Al-

varez-Mon, M., Sanz, E., and de la Hera, A. (1999). Multivalent structure of an alphabetaT cell receptor. Proc. Natl. Acad. Sci. USA *96*, 1547–1552.

Garcia, K.C., Degano, M., Stanfield, R.L., Brunmark, A., Jackson, M.R., Peterson, P.A., Teyton, L., and Wilson, I.A. (1996a). An αβ T cell receptor structure at 2.5 Å and its orientation in the TCR-MHC complex. Science *274*, 209–219.

Garcia, K.C., Scott, C.A., Brunmark, A., Carbone, F.R., Peterson, P.A., Wilson, I.A., and Teyton, L. (1996b). CD8 enhances formation of stable T-cell receptor/MHC class I molecule complexes. Nature *384*, 577–581.

Garcia, K.C., Tallquist, M.D., Pease, L.R., Brunmark, A., Scott, C.A., Degano, M., Stura, E.A., Peterson, P.A., Wilson, I.A., and Teyton, L. (1997). Alphabeta T cell receptor interactions with syngeneic and allogeneic ligands: affinity measurements and crystallization. Proc. Natl. Acad. Sci. USA *94*, 13838–13843.

Gimpl, G., Burger, K., and Fahrenholz, F. (1997). Cholesterol as modulator of receptor function. Biochemistry *36*, 10959–10974.

Grakoui, A., Bromley, S.K., Sumen, C., Davis, M.M., Shaw, A.S., Allen, P.M., and Dustin, M.L. (1999). The immunological synapse: a molecular machine controlling T cell activation. Science *285*, 221–227.

Hayashi, R.J., Loh, D.Y., Kanagawa, O., and Wang, F. (1998). Differences between responses of naive and activated T cells to anergy induction. J. Immunol. *160*, 33–38.

Iezzi, G., Karjalainen, K., and Lanzavecchia, A. (1995). The duration of antigenic stimulation determines the fate of naive and effector T cells. Immunity *8*, 89–95.

Janes, P.W., Ley, S.C., Magee, A.I., and Kabouridis, P.S. (2000). The role of lipid rafts in T cell antigen receptor (TCR) signalling. Semin. Immunol. *12*, 23–34.

Kabouridis, P.S., Janzen, J., Magee, A.L., and Ley, S.C. (2000). Cholesterol depletion disrupts lipid rafts and modulates the activity of multiple signaling pathways in T lymphocytes. Eur. J. Immunol. *30*, 954–963.

Kedl, R.M., Rees, W.A., Hildeman, D.A., Schaefer, B., Mitchell, T., Kappler, J., and Marrack, P. (2000). T cells compete for access to antigen-bearing antigen-presenting cells. J. Exp. Med. *192*, 1105–1113.

Kubo, R.T., Born, W., Kappler, J.W., Marrack, P., and Pigeon, M. (1989). Characterization of a monoclonal antibody which detects all murine αβ T cell receptors. J. Immunol. *142*, 2736–2742.

Lauffenburger, D.A., and Linderman, J.J. (1993). Receptors: Models for Binding, Trafficking, and Signaling (New York: Oxford University Press), pp. 133–180.

Monks, C.R.F., Freiberg, B.A., Kupfer, H., Sciaky, N., and Kupfer, A. (1998). Three-dimensional segregation of supramolecular activation clusters in T cells. Nature *395*, 82–86.

Montixi, C., Langlet, C., Bernard, A.M., Thimonier, J., Dubois, C., Wurbel, M.A., Chauvin, J.P., Pierres, M., and He, H.T. (1998). Engagement of T cell receptor triggers its recruitment to low-density detergent-insoluble membrane domains. EMBO J. *17*, 5334–5348.

Paul, W.E., and Seder, R.A. (1994). Lymphocyte responses and cytokines. Cell *76*, 241–251.

Perelson, A.S. (1984). In Cell Surface Dynamics: Concepts and Models, A.S. Perelson, C. Delisi, and F.W. Wiegel, eds. (New York: Marcel Dekker), pp. 223–276.

Rees, W., Bender, J., Teague, T.K., Kedl, R.M., Crawford, F., Marrack, P., and Kappler, J. (1999). An inverse relationship between T cell receptor affinity and antigen dose during Cd4+ T cell responses in vivo and in vitro. Proc. Natl. Acad. Sci. USA *96*, 9781–9786.

Reich, Z., Boniface, J.J., Lyons, D.S., Borochov, N., Wachtel, E.J., and Davis, M.M. (1997). Ligand-specific oligomerization of T-cell receptor molecules. Nature *387*, 617–620.

Savage, P.A., Boniface, J.J., and Davis, M.M. (1999). A kinetic basis for T cell receptor repertoire selection during an immune response. Immunity *10*, 485–492.

Schlueter, C.J., Manning, T.C., Schodin, B.A., and Kranz, D.M. (1996). A residue in the center of peptide QL9 affects binding to both L^d and the T cell receptor. J. Immunol. *157*, 4478–4485.

Schneck, J.P. (2000a). Monitoring antigen-specific T cells using MHC-Ig dimers. Immunol. Invest. *29*, 163–169.

Schneck, J.P., Slansky, J.E., O'Herrin, S.M., and Greten, T.F. (2000b). Monitoring antigen-specific T cells using MHC-Ig dimers. Curr. Protocols Immunol. Suppl. *35*, 17.2.1–17.2.17.

Simons, K., and Ikonen, E. (1997). Functional rafts in cell membranes. Nature *387*, 569–572.

Slansky, J.E., Rattis, F.M., Boyd, L.F., Fahmy, T., Jaffee, E.M., Schneck, J.P., Margulies, D.H., and Pardoll, D.M. (2000). Enhanced antigen-specific antitumor immunity with altered peptide ligands that stabilize the MHC-peptide-TCR complex. Immunity *13*, 529–538.

Sykulev, Y., Brunmark, A., Tsomides, T.J., Kageyama, S., Jackson, M., Peterson, P.A., and Eisen, H.N. (1994). High-affinity reactions between antigen-specific T-cell receptors and peptides associated with allogeneic and syngeneic major histocompatibility complex class I proteins. Proc. Natl. Acad. Sci. USA *91*, 11487–11491.

Sykulev, Y., Joo, M., Vturina, I., Tsomides, T.J., and Eisen, H.N. (1996). Evidence that a single peptide-MHC complex on a target cell can elicit a cytolytic T cell response. Immunity *4*, 565–571.

Sykulev, Y., Vugmeyster, Y., Brunmark, A., Ploegh, H.L., and Eisen, H.N. (1998). Peptide antagonism and T cell receptor interactions with peptide-MHC complexes. Immunity *9*, 475–483.

Udaka, K., Wiesmuller, K.-H., Kienle, S., Jung, G., and Walden, P. (1996). Self-MHC-restricted peptides recognized by an alloreactive T lymphocyte clone. J. Immunol. *157*, 670–678.

van der Merwe, P.A., Davis, S.J., Shaw, A.S., and Dustin, M.L. (2000). Cytoskeletal polarization and redistribution of cell-surface molecules during T cell antigen recognition. Semin. Immunol. *12*, 5–21.

Viola, A., Schroeder, S., Sakakibara, Y., and Lanzavecchia, A. (1999). T lymphocytes costimulation mediated by reorganization of membrane microdomains. Science *283*, 680–682.

Wang, J., Lim, K., Smolyar, A., Teng, M., Liu, J., Tse, A.G., Liu, J., Hussey, R.E., Chishti, Y., Thomson, C.T., et al. (1998). Atomic structure of an alphabeta T cell receptor (TCR) heterodimer in complex with an anti-TCR fab fragment derived from a mitogenic antibody. EMBO J. *17*, 10–26.

Willcox, B.E., Gao, G.F., Wyer, J.R., Ladbury, J.E., Bell, J.I., Jakobsen, B.K., and van der Merwe, P.A. (1999). TCR binding to peptide-MHC stabilizes a flexible recognition interface. Immunity *10*, 357–365.

Wofsy, C., and Goldstein, B. (1992). Interpretation of Scatchard plots for aggregating receptor systems. Math Biosci. *112*, 115–154.

Wyer, J.R., Willcox, B.E., Gao, G.F., Gerth, U.C., Davis, S.J., Bell, J.I., van der Merwe, P.A., and Jakobsen, B.K. (1999). T cell receptor and coreceptor CD8αα bind peptide-MHC independently and with distinct kinetics. Immunity *10*, 219–225.

Xavier, R., Brennan, T., Li, Q., McCormack, C., and Seed, B. (1998). Membrane compartmentation is required for efficient T cell activation. Immunity *8*, 723–732.